Miniaturized Microstrip Cross-Coupled Filters Using Quarter-Wave or Quasi-Quarter-Wave Resonators

Cheng-Chung Chen, Yi-Ru Chen, and Chi-Yang Chang, *Member, IEEE*

***Abstract*—Miniaturized microstrip filters using quarter-wave or quasi-quarter-wave resonators with cross-coupling are presented. The quarter-wavelength resonators enable very compact positively or negatively cross-coupled filters to be realized. The combination of quarter-wave and quasi-quarter-wave resonators facilitates the cross-coupling with a proper coupling phase. A new explanation for the coupling phase between the main-coupling and cross-coupling paths is proposed. Different filters that use the proposed resonators are realized and may have either quasi-elliptical or flat group-delay responses. Measurement results correlate well with theoretical predictions.**

***Index Terms*—Microstrip cross-coupled filter, miniaturized filter, Quarter-wave resonator, quasi-quarter-wave resonator.**

I. Introduction

THE quarter-wave resonators are frequently used in interdigital filters [1]. Conventional interdigital filters can be very compact, but most exhibit the Chebyshev or Butterworth response. Recently, cross-coupled filters have attracted much attention due to their quasi-elliptical or flat group-delay responses. Many cross-coupled microstrip filters have been reported [2], [5]–[13]. Most of them, however, use half-wave resonators. The quarter-wavelength interdigital-type filter is attractive because it is more compact than a conventional cross-coupled filter with half-wave resonators. The cross-coupled filter, using quarter-wavelength resonators, was first introduced in [2], where the nonadjacent coupling between quarter-wave resonators was realized with an appropriately positioned slot in the dual-plane configuration.

This paper presents a novel single-plane filter structure that is suitable for realizing either a trisection [5]–[7] or a cascade quadruplet (CQ) [8]–[13] quarter-wavelength interdigital filter, as shown in Fig. 1. The first and last quarter-wave resonators are bent to achieve cross-coupling. In addition, the bending of the resonators is such that the coupling electrical length between the resonators in the main-coupling path is less than 90°. The spacing between the resonators should be closer than that of the resonators with a coupling length of 90°. Thus, the filter is made more compact than the conventional interdigital filter. The resonators in Fig. 1 are conventional quarter-wave resonators with one end grounded. Unfortunately, they have two shortcomings.

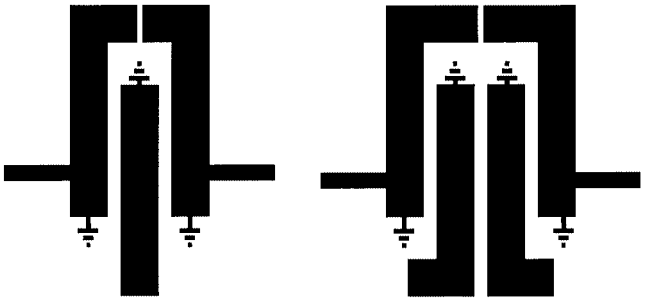

(a) (b)

Fig. 1. (a) Trisection filter with three quarter-wave resonators. (b) CQ filter with four quarter-wave resonators.

The first shortcoming is that the trisection filter in Fig. 1(a) can have a transmission zero only at the lower stopband, and the CQ filter in Fig. 1(b) can have only a quasi-elliptical response. The filter structure constrains the cross-coupling to be a capacitive microstrip gap. The trisection filter with the upper stopband transmission zero or a CQ filter with flat group-delay response cannot be realized with the filter structures in Fig. 1. The applications of the proposed cross-coupled filter are limited accordingly.

The second shortcoming is that the frequency of the transmission zeros of the filters shown in Fig. 1 drifts considerably. This phenomenon was reported in [9]. The drift of transmission zeros is much greater in quarter-wave resonator filters than in half-wave resonator filters. More seriously, this phenomenon destroys the flat group-delay property of a linear phase CQ filter, as discussed in Section III.

This paper proposes the following methods to solve these problems.

A. Quasi-Quarter-Wave Resonator

In contrast to the quarter-wave resonator depicted in Fig. 2(a), a novel resonator is proposed, as shown in Fig. 2(b). It is referred to herein as a quasi-quarter-wave resonator because its physical shape is that of a quarter-wave resonator, except for the narrow slot at the center of strip. The above two problems can be solved using this new resonator. The quasi-quarter-wave resonator includes a pair of tightly coupled lines that are connected at one end. The electrical behavior of this quasi-quarter-wave resonator closely resembles that of a conventional quarter-wave resonator, except that the real ground in Fig. 2(a) is changed into a virtual ground in Fig. 2(b) at the fundamental resonant frequency. Moreover, the size of the quasi-quarter-wave resonator

Manuscript received October 30, 2001; revised March 26, 2002. This work was supported in part by the Ministry of Education, Taiwan, R.O.C., under Contract 89-E-FA06-2-4.

C.-C. Chen and C.-Y. Chang are with the Institute of Electrical Communication Engineering, National Chiao Tung University, Hsinchu, Taiwan 30050, R.O.C.

Y.-R. Chen was with the Institute of Electrical Communication Engineering, National Chiao Tung University, Hsinchu, Taiwan 30050, R.O.C. She is now with Euvis Inc., Westlake Village, CA 91362 USA.

Digital Object Identifier 10.1109/TMTT.2002.806924

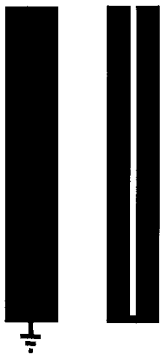

(a) (b)

Fig. 2. (a) Quarter-wave resonator. (b) Quasi-quarter-wave resonator.

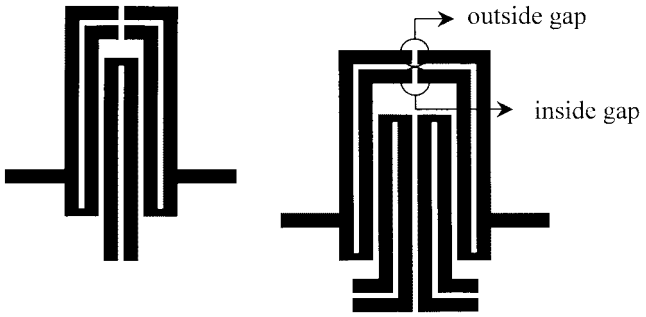

(a) (b)

Fig. 3. (a) Trisection filter with three quasi-quarter-wave resonators. (b) CQ filter with four quasi-quarter-wave resonators.

is similar to that of the quarter-wave resonator and can be bent to achieve cross-coupling.

The concept of the quasi-quarter-wave resonator was introduced to realize alternative versions of conventional interdigital and combline filters in [3] and [4]. At the fundamental resonant frequency, the voltage distribution of a quasi-quarter-wave resonator is in the odd mode with respect to that central plane, while the quarter-wave resonator is in the even mode. Therefore, the quasi-quarter-wave and quarter-wave resonators exhibit a 180° phase difference when coupled with other resonators. This property can be used to realize the specified coupling phase in both CQ and trisection filters presented in this paper.

B. Combining Quarter-Wave and Quasi-Quarter-Wave Resonators

This newly proposed quasi-quarter-wave resonator can be used to realize filters similar to those proposed in Fig. 1, as shown in Fig. 3. Unfortunately, a CQ filter still encounters the first problem if it uses only the quasi-quarter-wave resonators. Nevertheless, a CQ filter with flat group delay can be realized by properly combining the quarter-wave and quasi-quarter-wave resonators. For example, if one resonator differs from the others, then the main-coupling phase changes by 180° with respect to the cross-coupling phase. Therefore, all kinds of trisection filters or CQ filters can be realized.

Another important difference between a filter with a quasi-quarter-wave resonator and one with a quarter-wave resonator is that the second problem of frequency drifting of transmission zeros can be compensated if the input and output resonators are quasi-quarter-wave resonators, as will be discussed in Section III.

II. Filter Response Analysis

CQ filters with quasi-elliptical or flat group-delay response are realized by cross-couplings between the first and fourth resonators. In the prototype circuit, cross-coupling is represented by an admittance inverter. The quasi-elliptical response can be achieved by a negative admittance inverter, whereas the flat group-delay response can be achieved by a positive admittance inverter [15]. Physically, the opposite sign of the admittance inverter denotes whether the main-coupling and cross-coupling paths are in-phase or out-of-phase. In the literature [8]–[13], microstrip cross-coupled filters based on square open-loop resonators or hairpin resonators have been proposed to realize both quasi-elliptical and linear phase responses. In that research, magnetic coupling and electric coupling between resonators were arranged to realize in-phase and out-of-phase cross-coupling. In the case of the trisection filter, a negative admittance inverter between two nonadjacent resonators of an asynchronously tuned three-pole filter causes a lower stopband transmission zero, whereas a positive admittance inverter between two nonadjacent resonators causes an upper stopband transmission zero. In [7], electric or magnetic couplings between two open-loop resonators are employed to realize the positive or negative admittance inverter, respectively, in the prototype circuit. Briefly, most works has been limited to the arrangement of open-loop or hairpin resonators to realize electric, magnetic, or mixed coupling. In-phase and out-of-phase coupling between the main-coupling path and the cross-coupling path, which were explained in [6]–[13] as electric and magnetic coupling, cannot be applied to the filters proposed in this paper. Thus, a clear rule governing the design of the cross-coupled filters as presented here is desired.

A new explanation of the involvement of coupling phase in a cross-coupled filter is given. The phase relationship between the main-coupling path and the cross-coupling path of the proposed filter configurations are analyzed for frequencies below and above the passband center frequency f_0. A circuit simulator, such as Microwave Office, can analyze the difference in phase between the main-coupling path and the cross-coupling path. The phase analysis shows that a CQ filter responds quasi-elliptically if the phase difference between the main-coupling and cross-coupling paths is 180° over both frequency ranges $f < f_0$ and $f > f_0$, whereas a CQ filter exhibits flat group-delay response if the phase difference between the main-coupling and cross-coupling paths is 0° over both frequency ranges $f < f_0$ and $f > f_0$. As well as a CQ filter, a trisection filter has a lower stopband transmission zero if the phase difference between the main-coupling and cross-coupling path is 180° when $f < f_0$ and 0° when $f > f_0$. Similarly, a trisection filter has a higher stopband transmission zero if the phase difference between the main-coupled and the cross-coupled paths is 0° when $f < f_0$ and 180° when $f > f_0$.

The coupling between each resonator was examined to further understand the coupling phase of both the main-coupling and cross-coupling paths for the proposed filter configuration. Fig. 4

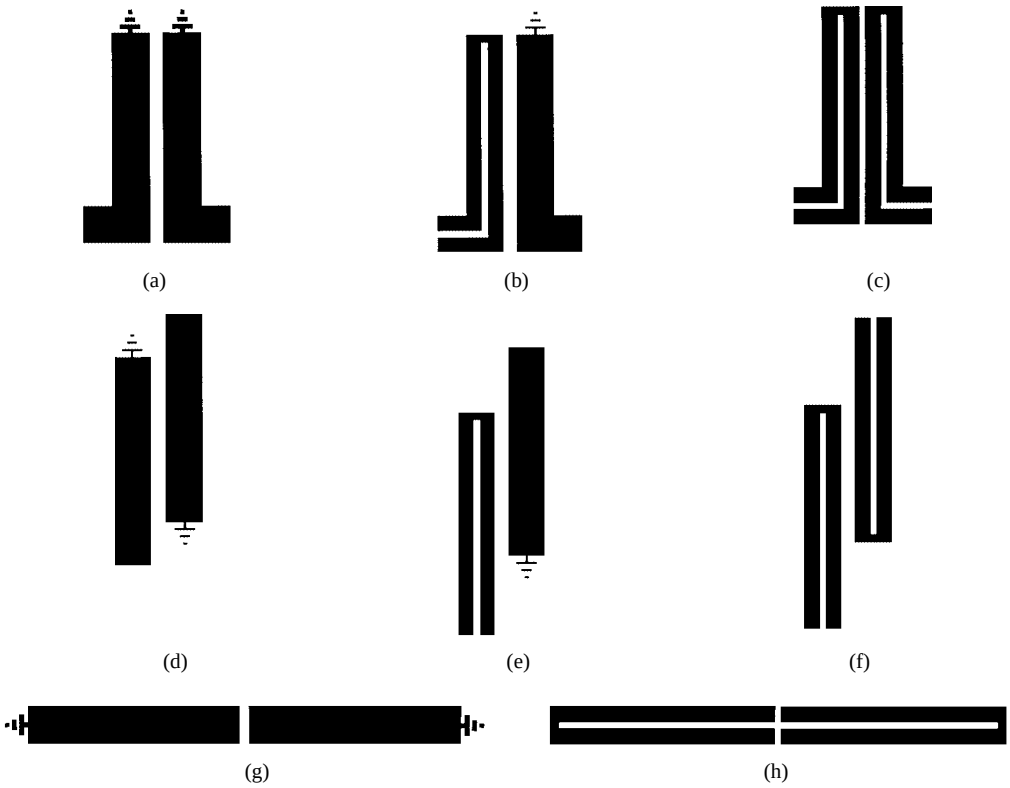

Fig. 4. (a)–(h) Basic coupling structures used in the proposed filters.

illustrates the eight basic coupling structures used here. The circuits in Fig. 4 all consist of quarter-wave or quasi-quarter-wave resonators and are in comb-type coupling, interdigital-type coupling, or capacitive gap-type coupling arrangements. The circuit simulator is employed here to determine the frequency response of voltage amplitude and phase in each coupling structure. Fig. 5 shows eight schematics circuits used to simulate each coupling structure. In all of the schematic circuits, a voltage source is coupled to one of two resonators via a coupling capacitor. The quasi-quarter-wave resonator is represented by a coupled-line model. The resonant frequency f_0 is normalized to 1 GHz. Two voltmeters are connected to each resonator at specified positions to measure the frequency response of the amplitude and phase. Fig. 6 shows the simulated phase and amplitude response of each coupling structure, corresponding to Fig. 5.

Some important features should be emphasized. As an example, take Fig. 6(a). This figure depicts the amplitude and phase responses of two quarter-wave resonators coupled with a comb-type coupling structure. The dashed line is the voltage response of the resonators and includes two resonant peaks at f_1 and f_2. The voltage magnitude and the frequency location of the resonant peaks depends on the internal and external coupling strength. The solid line represents the phase responses of each resonator. The simulated result indicates that the output voltage is in-phase when $f < f_0$ and 180° out-of-phase when $f > f_0$ with respect to the input voltage. Interestingly, changing the even- and odd-mode impedance Zoe and Zoo or the coupling length between two coupled resonators in the referent schematic circuit causes the position of two resonant peaks to change accordingly, while the phase differences below and above the center frequency remain unchanged. A similar phenomenon exists in the other seven coupling structures in Fig. 5, as shown in the remaining part of Fig. 6. In summary, the coupling phase is 0° when $f < f_0$ and 180° when $f > f_0$ if any two resonators are arranged in a comb-type coupling. The coupling phase is 180° when $f < f_0$ and 0° when $f > f_0$ if any two resonators are arrange in interdigital-type coupling. The coupling phases presented in Fig. 6 are useful in explaining the response of the cross-coupled filters proposed here.

Table I displays some possible configurations of filters constructed by quarter-wave and/or quasi-quarter-wave resonators. Using the phase response presented in Fig. 6, the filtering properties of cross-coupled filters in Table I can be determined by comparing the phase shift between the main-coupling and cross-coupling paths. The phase shift of the main-coupling path is determined by summing the phase shifts in each coupling structure. As an example, consider the CQ filter specified in Table I(b). According to Fig. 6(d), the phase shift between two interdigital-coupled quarter-wave resonators is 180° when $f < f_0$ and 0° when $f > f_0$, implying that a 180° phase shift exists when $f < f_0$ and a 0° phase shift exists when $f > f_0$ between the first and second resonators and between the third and fourth resonators. Again, from Fig. 6(a), the phase shift between the second and third resonators, which is a comb-type coupling, is 0° when $f < f_0$ and 180° when $f > f_0$, implying that the total phase shift of the main-coupling path is 0° when $f < f_0 (180 + 0 + 180 = 360 = 0^\circ)$ and 180° when $f > f_0 (0 + 180 + 0 = 180^\circ)$. However, the phase shift along the cross-coupling path, which constitutes a capacitive gap-type coupling, is 180° when $f < f_0$ and 0° when $f > f_0$. Briefly, the phase difference between the main-coupling path and the

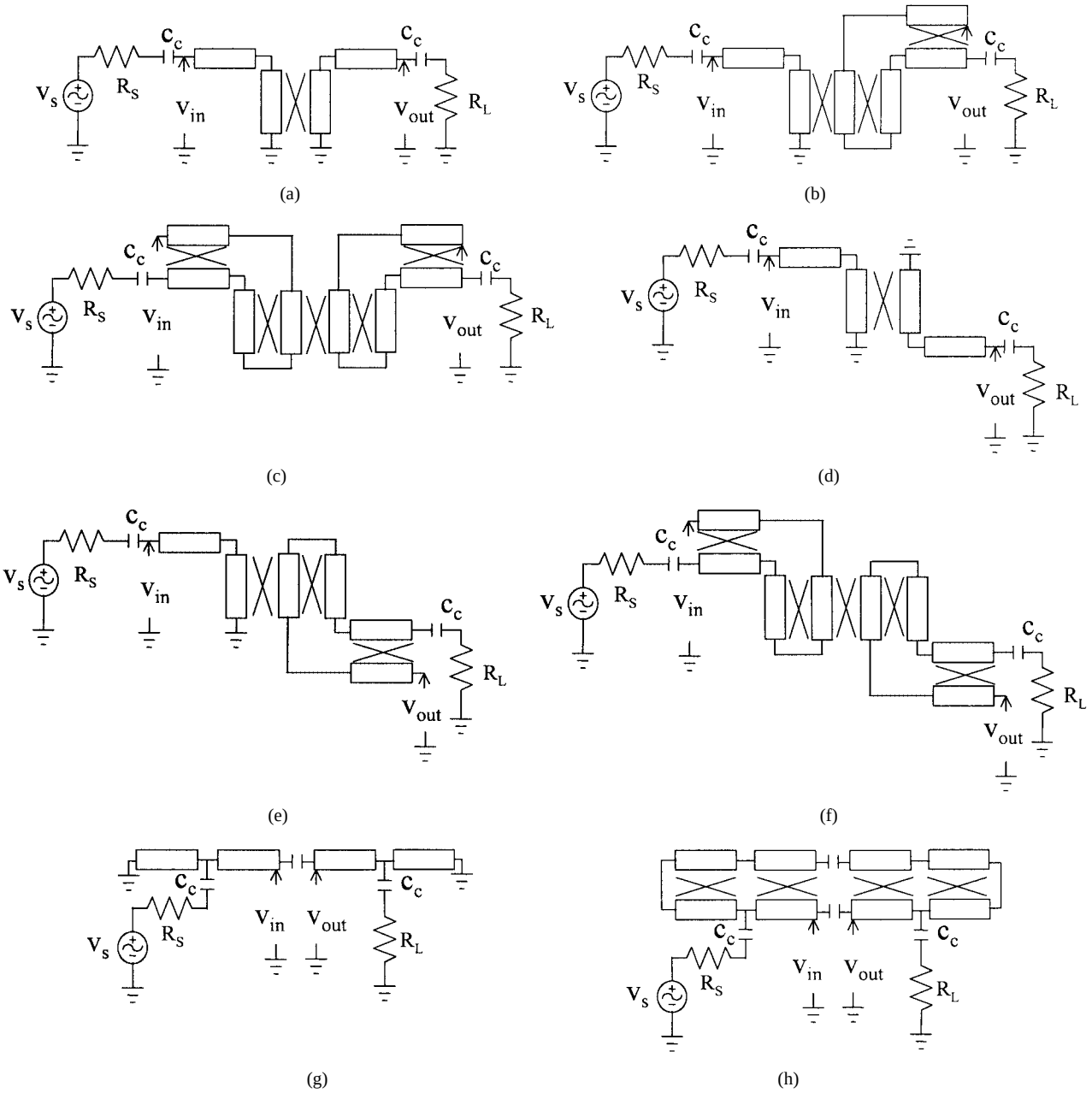

Fig. 5. Schematic circuits used to simulate the frequency responses of two resonators in each coupling structure of Fig. 4(a)–(h).

cross-coupling path is 180° at frequencies below or above the center frequency. Accordingly, the voltages will cancel each other if the coupling amplitude of main-coupling path equals that of the cross-coupling path. Therefore, a transmission zero occurs. Consequently, the CQ filter that uses four quarter-wave resonators, as shown in Table I(b), responds quasi-elliptically.

Following the above discussion, a CQ filter with a flat group-delay response can be obtained if the phase difference between the main coupling and cross-coupling is 0° below and above the center frequency. Changing the total phase shift along the main-coupling path by 180° causes the phase difference between the main-coupling and cross-coupling paths to become 0°. Hence, the response of this CQ filter becomes a flat group delay, which can be realized by replacing the second quarter-wave resonator of the CQ filter in Table I(b) with a quasi-quarter-wave resonator. The quasi-quarter-wave resonator causes a further phase shift of 180° when coupling with other resonators. The main-coupling and cross-coupling paths of the filter then become in-phase at frequencies below and above the center frequency. Consequently, the filter should be a flat group-delay filter. Table I(d) gives the circuit configuration of this CQ filter. Switching any one of the quarter-wave resonators in Table I(b) to a quasi-quarter-wave resonator causes the filter to exhibit a flat group-delay response.

The same analysis can also be applied to determine the location of the transmission zero of a trisection filter. For example, the filter presented in Table I(h) is a trisection filter with three quarter-wave resonators, OR Fig. 6(d) shows that the phase shift is 180° when $f < f_0$ and 0° when $f > f_0$, both between the first and second resonators and between the second and third res-

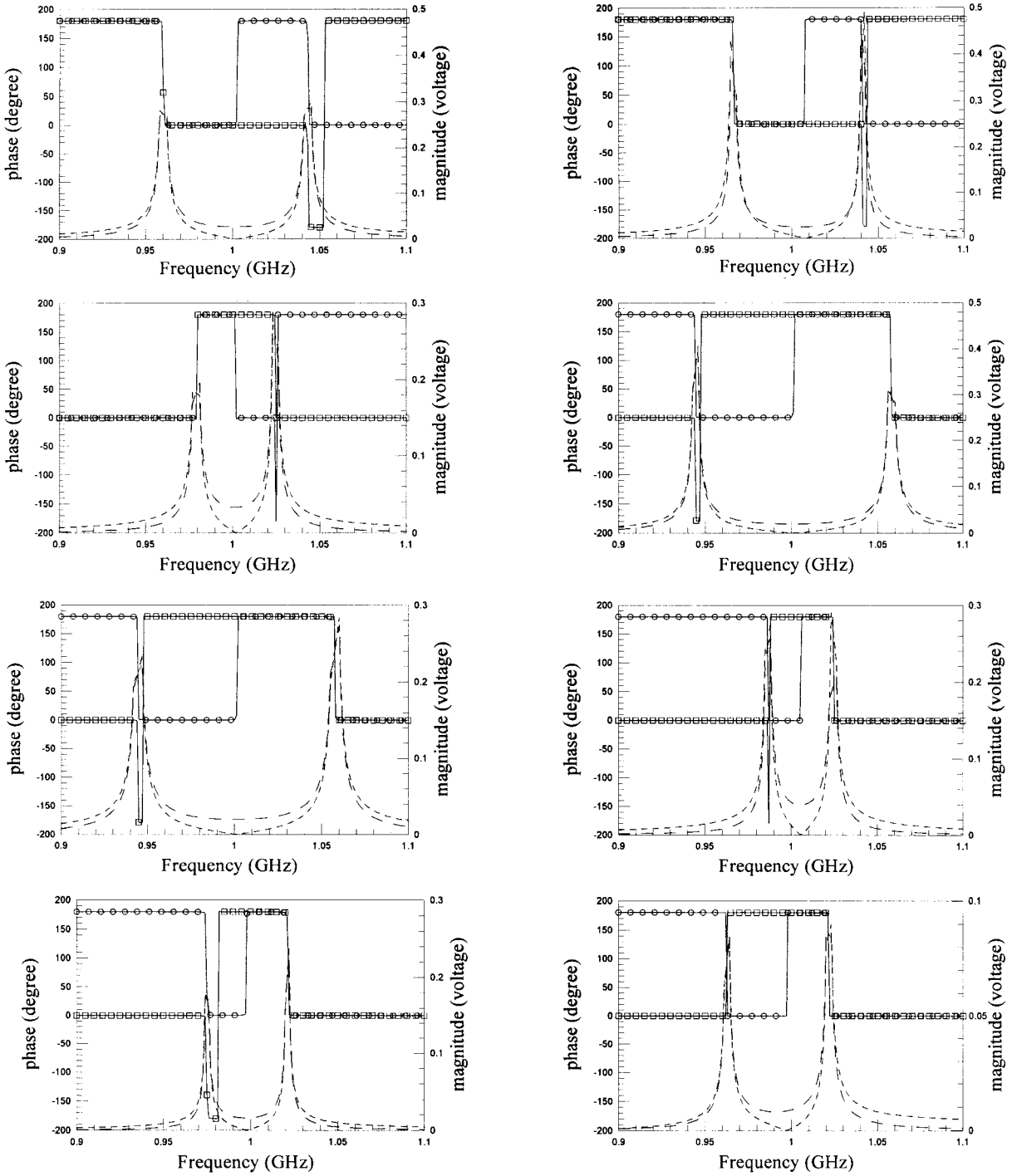

Fig. 6. Frequency responses of V_{out} and V_{in} of the coupling structures of Fig. 5(a)–(h). – – – – – – – – – – V_{in} (magnitude) – – – – – – – – V_{out} (magnitude) ⊖⊖⊖ V_{in} (phase) ⊟⊟⊟ V_{out} (phase).

onators. Thus, the total phase shift through the main-coupling path is 0° at frequencies $f < f_0$ and $f > f_0$. From Fig. 6(g), the phase shift through the cross-coupling path is 180° when $f < f_0$ and 0° when $f > f_0$. Hence, the phase difference between the main-coupling and cross-coupling paths of this trisection filter is 180° when $f < f_0$ and 0° when $f > f_0$. Therefore, the filter has a transmission zero in the lower stopband. As for the CQ filter, replacing the second quarter-wave resonator by a quasi-quarter-wave resonator, as shown in Table I(f), causes the total phase shift along the main-coupling path to change by 180° at frequencies above and below the center frequency. Thus, the main-coupling and cross-coupling paths are in-phase when $f < f_0$ and 180° out-of-phase when $f > f_0$. Consequently, the trisection filter in Table I(f) has a transmission zero in the upper stopband.

The method described above is applied to derive the phase difference of each filter specified in Table I. The corresponding response is the relevant row in the table.

TABLE I
PHASE DIFFERENCE BETWEEN MAIN-COUPLING AND CROSS-COUPLING OF BOTH TRISECTION FILTERS AND CQ FILTERS, AND CORRESPONDING RESPONSES

Filter configurations	Frequency concerned	Relation between nodes		Phase difference	Total sum	Frequency response predicted
(a) 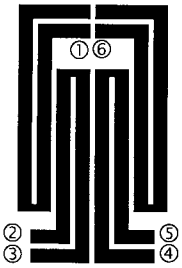	>fo	①	②	0	180	
		②	③	180		
		③	④	180		
		④	⑤	180		
		⑤	⑥	0		
		①	⑥	0	0	
	< fo	①	②	180	0	
		②	③	180		
		③	④	0		
		④	⑤	180		
		⑤	⑥	180		
		①	⑥	180	180	
(b) 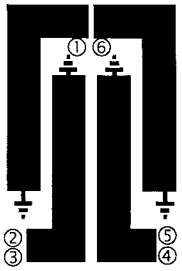	> fo	①	②	0	180	
		②	③	0		
		③	④	180		
		④	⑤	0		
		⑤	⑥	0		
		①	⑥	0	0	
	< fo	①	②	180	0	
		②	③	0		
		③	④	0		
		④	⑤	0		
		⑤	⑥	180		
		①	⑥	180	180	
(c) 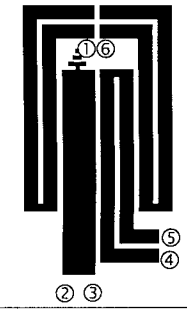	> fo	①	②	0	0	 flat group delay
		②	③	0		
		③	④	180		
		④	⑤	180		
		⑤	⑥	0		
		①	⑥	0	0	
	< fo	①	②	180	180	
		②	③	0		
		③	④	0		
		④	⑤	180		
		⑤	⑥	180		
		①	⑥	180	180	
(d) 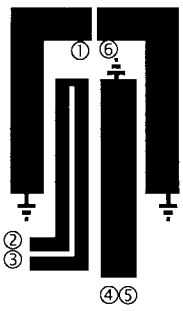	> fo	①	②	0	0	 flat group delay
		②	③	180		
		③	④	180		
		④	⑤	0		
		⑤	⑥	0		
		①	⑥	0	0	
	< fo	①	②	180	180	
		②	③	180		
		③	④	0		
		④	⑤	0		
		⑤	⑥	180		
		①	⑥	180	180	

III. COMPENSATION OF DRIFT OF TRANSMISSION ZEROS

The drift of transmission zeros is encountered in many microstrip cross-coupled filters. The frequency drifting in the proposed filters can be compensated for when the first and last resonators are quasi-quarter-wave resonators.

Two coupling gaps, the outside and the inside gaps in Fig. 3(b), exist between the first and last resonators when they are quasi-quarter-wave resonators. The outside gap causes the transmission zeros to drift to lower frequency, while the inside gap causes the transmission zeros to drift to higher frequency. The drift of the transmission zeros can be compensated for by

TABLE I *(Continued.)*
PHASE DIFFERENCE BETWEEN MAIN-COUPLING AND CROSS-COUPLING OF BOTH TRISECTION FILTERS AND CQ FILTERS, AND CORRESPONDING RESPONSES

Structure of the filter	Frequency concerned	Relation between nodes		Phase difference	Total sum	Frequency response predicted
(e) 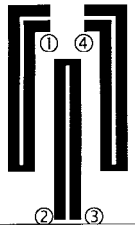	>fo	①	②	0	180	
		②	③	180		
		③	④	0		
		①	④	0	0	
	<fo	①	②	180	180	
		②	③	180		
		③	④	180		
		①	④	180	180	
(f) 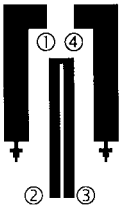	> fo	①	②	0	180	
		②	③	180		
		③	④	0		
		①	④	0	0	
	< fo	①	②	180	180	
		②	③	180		
		③	④	180		
		①	④	180	180	
(g) 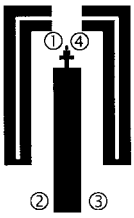	> fo	①	②	0	0	
		②	③	0		
		③	④	0		
		①	④	0	0	
	< fo	①	②	180	0	
		②	③	0		
		③	④	180		
		①	④	180	180	
(h) 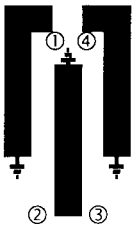	> fo	①	②	0	0	
		②	③	0		
		③	④	0		
		①	④	0	0	
	< fo	①	②	180	0	
		②	③	0		
		③	④	180		
		①	④	180	180	

appropriately distributing the outside and inside gap-capacitance while maintaining a constant total gap-capacitance. This procedure can be empirically implemented. The simulated results imply that the drift of the transmission zeros is negligible if they are very close to the passband. In the filter with the flat group-delay response, no adjustment is required since the real axis zero is normally very close to unity.

The situation becomes much more serious when the first and last resonators are quarter-wave resonators, in that the drift of the transmission zeros is greater and the compensation method described above is ineffective. Importantly, quarter-wave resonators should not be used as input and output resonators when a CQ filter with flat group-delay response is required. Section IV shows an example to demonstrate the situation.

IV. DESIGN EXAMPLES

The quarter-wave and quasi-quarter-wave resonators used here are built on a Rogers RO4003 substrate. The substrate has a relative dielectric constant of 3.38, a thickness of 20 mil, and a copper cladding of 0.5 oz. The linewidth of the quarter-wave resonator is 100 mil. The total linewidth of a quasi-quarter-wave resonator is also selected as 100 mil. The slot in the quasi-quarter-wave resonator is 8 mil. Consequently, the physical shape of a quarter-wave resonator is the same as that of a quasi-quarter-wave resonator, except for presence of the 8-mil slot.

A. CQ Filters

Four CQ filters corresponding to Table I(a)–(d) are designed to validate the filter configurations presented in this paper. The low-pass prototype parameters of the CQ filters are synthesized by the method described in [16]. The CQ filter with voltage standing-wave ratio (VSWR) of 1.2, fractional bandwidth of 5%, and a real frequency transmission zero pair at $\pm j1.5$ is designed to respond quasi-elliptically. The CQ filter with VSWR of 1.3, fractional bandwidth of 5%, and a real axis transmission zero pair at ± 1.05 is designed to exhibit the flat group-delay response. Table II lists the design parameters of the bandpass filters.

A full-wave electromagnetic (EM) simulator from Sonnet 6.0a[1] is used to calculate the two resonant peaks of the corre-

[1]Sonnet 6.0a, Sonnet Software Inc., Liverpool, NY.

TABLE II
DESIGN PARAMETERS OF CQ BANDPASS FILTERS

CQ Filter	K12	K23	K34	K14	Qe1	Qe4
Transmission zero at ±j1.5, VSWR=1.2, FBW=5%	0.04106	0.04248	0.04106	-.01874	18.747	18.747
Transmission zero at ±1.05, VSWR=1.3, FBW=5%	0.04416	0.02656	0.04416	0.01506	19.816	19.816

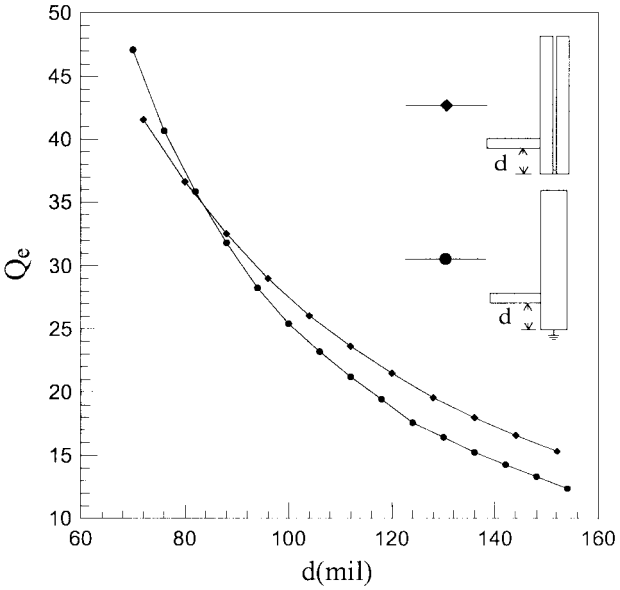

Fig. 7. Calculated external quality factors of both quarter-wave and quasi-quarter-wave resonators.

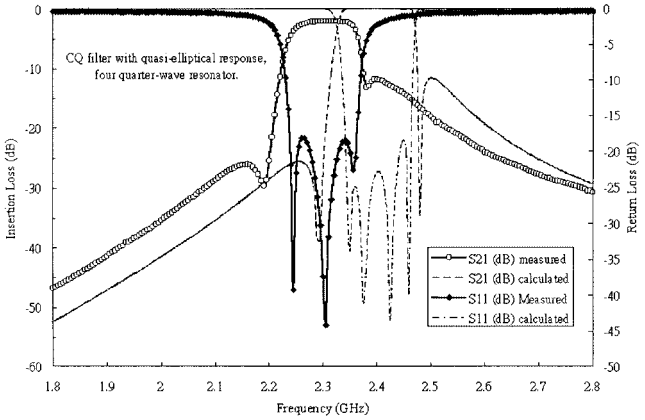

(a)

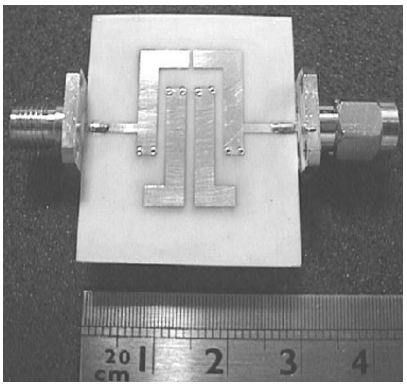

(b)

Fig. 8. CQ filter in Table I(b). (a) Measured and calculated frequency responses. (b) Photograph of the filter

sponding coupling structure and, thus, determine the coupling coefficient of the resonators. The coupling coefficient is obtained from two eigenfrequencies f_1 and f_2 given as follows:

$$k_{i,j} = \frac{f_2^2 - f_1^2}{f_2^2 + f_1^2} \tag{1}$$

where $k_{i,j}$ represents the coupling coefficient between the ith and jth resonators.

The external quality factor is obtained from the phase and group delay of S_{11} according to the method described in [17]. Here, the input/output 5-Ω microstrip line is taped to the first and last resonators as the external coupling structure. Fig. 7 presents the calculated external quality factors of both quarter-wave and quasi-quarter-wave resonators. It is noted that the effect of the bending of the resonator on the tap position is negligible.

Fig. 8(a) shows the measured and calculated results for the CQ filter with four quarter-wave resonators [the filter shown in Table I(b)]. Asymmetric transmission zeros are observed on both sides of the stopband. Both transmission zeros drift toward low frequency. In particular, the lower transmission zero drifts to a much lower frequency than that original specified frequency. A circuit simulator is used to simulate the cross-coupled filter with four quarter-wave resonators to further investigate this phenomenon. Following a method similar to that described in Section II, the phase difference between the main-coupling and cross-coupling paths is 180° on both sides of the passband, as expected, but the amplitude crossover frequencies of the main-coupling and cross-coupling paths are asymmetrically on two sides of the stopband. Consequently, the two transmission zeros of a CQ filter are not symmetric with the passband. Fig. 8(b) presents a photograph of this filter.

As stated in Section III, the filter that uses quasi-quarter-wave resonators is a better choice than the one that uses quarter-wave resonators to give a cross-coupled filter with two symmetric transmission zeros. Fig. 9(a) presents the measured and calculated results of the filter in Table I(a) that uses four quasi-quarter-wave resonators. After an adjustment of the outside and inside gaps between the input and output resonators, two finite frequency transmission zeros are symmetrically located with respect to the passband, as theoretically predicted. Fig. 9(b) presents a photograph of this filter.

Fig. 10(a) gives the measured and calculated results for the CQ filter in Table I(c) with three quasi-quarter-wave resonators and one quarter-wave resonator. The attenuation skirt is not as sharp as an ordinary four-pole Chebyshev filter. However, the filter shows better passband group-delay characteristics than the Chebyshev filter. Fig. 10(b) shows the measured group delays of this CQ linear-phase filter and a four-pole Chebyshev filter with the same bandwidth and passband ripple. The group delay in the passband of the CQ filter is flattened due to the introduction of real axis transmission zeros. Fig. 10(c) presents a photograph of the filter.

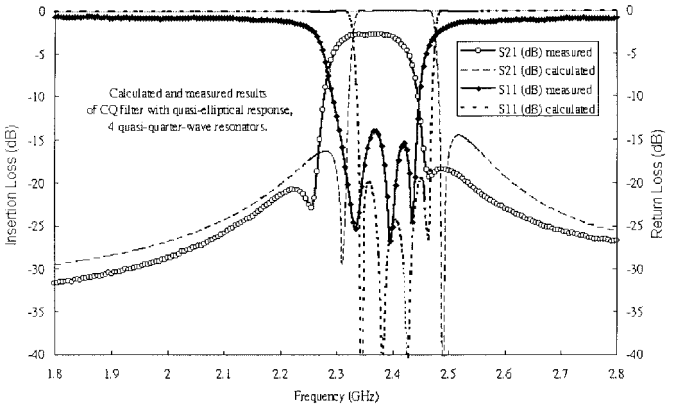

(a)

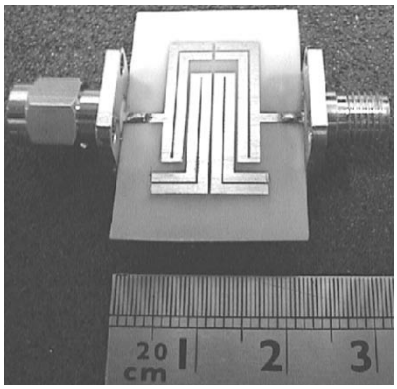

(b)

Fig. 9. CQ filter in Table I(a). (a) Measured and calculated frequency responses. (b) Photograph of the filter.

Fig. 11 gives the measured and calculated results for another CQ filter with a flat group-delay response. The filter in Table I(d) consists of three quarter-wave resonators and one quasi-quarter-wave resonator. As discussed in Section III, the passband group delay of this filter is not at all flat because the input/output resonators are quarter-wave resonators. Notably, no compensation could be performed for this filter to improve the group-delay response. Briefly, if a filter with a flat group-delay response is required, then the filter structure in Table I(c) should be used.

B. Trisection Filters

This paper considers four configurations of trisection filters, as shown in Table I(e)–(h). Two trisection filters in Table I(g) and (h) have a lower stopband finite frequency transmission zero at $-j2.5$, while the other two trisection filters in Table I(e) and (f) have an upper stopband finite frequency transmission zero at $+j2.5$. The filters have the following parameters. The passband ripple is 0.1 dB, the fractional bandwidth is 5%, and the center frequency is 2.4 GHz. The low-pass prototype parameters of trisection filters are synthesized according to the method described in [18], [19]. Table III lists the prototype element values and design parameters for bandpass filters. The procedures for determining the coupling coefficient and external Q value are similar to those for determining the corresponding parameters for the CQ filter. The trisection filters are fabricated on the same substrate as the CQ filters.

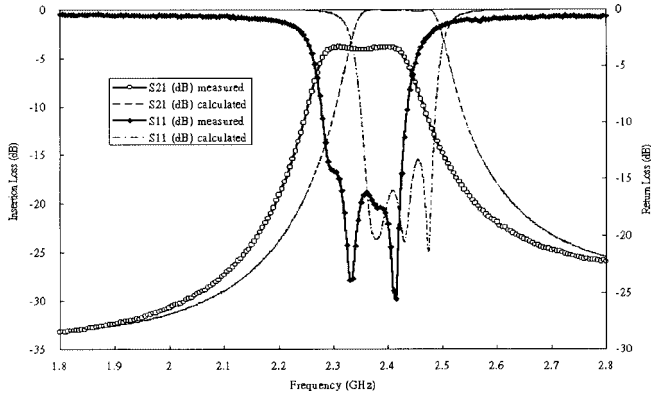

(a)

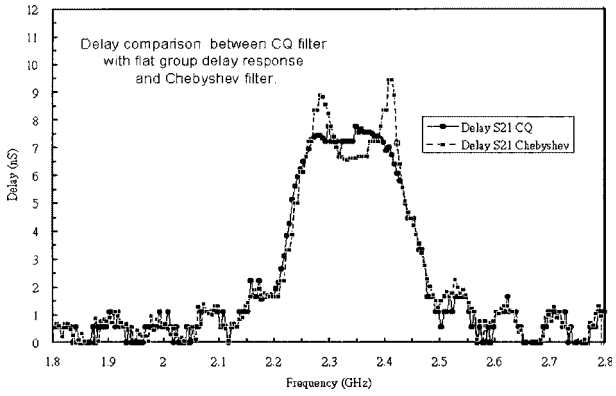

(b)

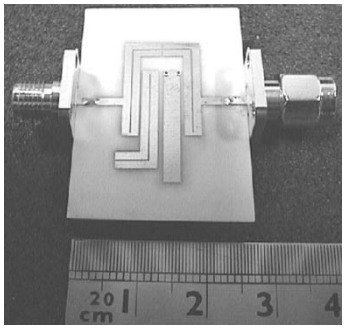

(c)

Fig. 10. CQ filter in Table I(c). (a) Measured and calculated frequency responses. (b) Measured group-delay comparison of this CQ filter to a Chebyshev filter with four quasi-quarter-wave resonators. (c) Photograph of the filter.

Fortunately, the transmission zero drift in the trisection filters can be compensated for by adjusting the cross-coupling gap, even when the input and output resonators are quarter-wave resonators.

Fig. 12 presents the measured and calculated results of the trisection filter in Table I(h) with three quarter-wave resonators. As listed in Table I, a finite frequency transmission zero occurs in the lower stopband.

Fig. 13 presents the measured results for the trisection filter in Table I(f) with two quarter-wave resonators and one quasi-quarter-wave resonator. Replacing the second quarter-wave resonator in Table I(h) with a quasi-quarter-wave resonator causes the finite frequency transmission zero to change from the lower to upper stopband in a manner consistent with this analysis. However, the lower stopband includes

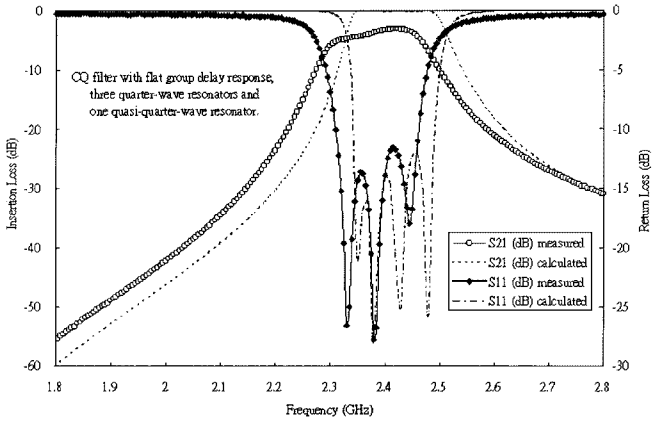

(a)

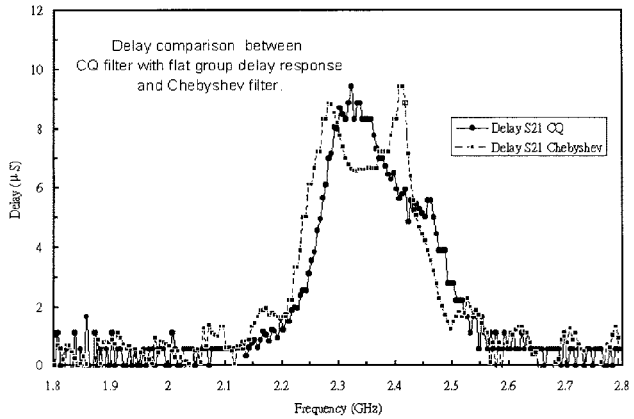

(b)

Fig. 11. CQ filter in Table I(d). (a) Measured and calculated frequency responses. (b) Measured group-delay comparison of this CQ filter to a Chebyshev filter with four quasi-quarter-wave resonators.

TABLE III
DESIGN PARAMETERS OF TRISECTION BANDPASS FILTERS

Transmission zero at –j2.5, 0.1 dB ripple, FBW=5% and f_0=2.4GHz					
Resonator	g_i	B_i	J_{ij}	$F_{res,i}$	k_{ij}
1	0.16412	-0.08305		2.40484	
2	0.20550	0.47750		2.37791	
3	0.16412	-0.08305		2.40484	
1-2			1.0		0.04333
2-3			1.0		0.04333
1-3			-0.36356		-0.01764
Transmission zero at–j2.5, 0.1 dB ripple, FBW=5% and f_0=2.4GHz					
Resonator	g_i	B_i	J_{ij}	$F_{res,i}$	k_{ij}
1	0.16412	0.08305		2.39517	
2	0.20550	-0.47750		2.42229	
3	0.16412	0.08305		2.39517	
1-2			1.0		0.04333
2-3			1.0		0.04333
1-3			0.36356		-0.01764

an extra transmission zero due to parasitic magnetic coupling between the first and third quarter-wave resonators. Unlike electric coupling, the magnetic coupling between the first and third resonators causes a transmission zero in the lower stopband.

Fig. 14 presents the measured results for the trisection filter in Table I(e) with three quasi-quarter-wave resonators. A finite frequency transmission zero occurs in the upper stopband.

Fig. 15 shows the measured results for the trisection filter in Table I(g) with two quasi-quarter-wave resonators and one

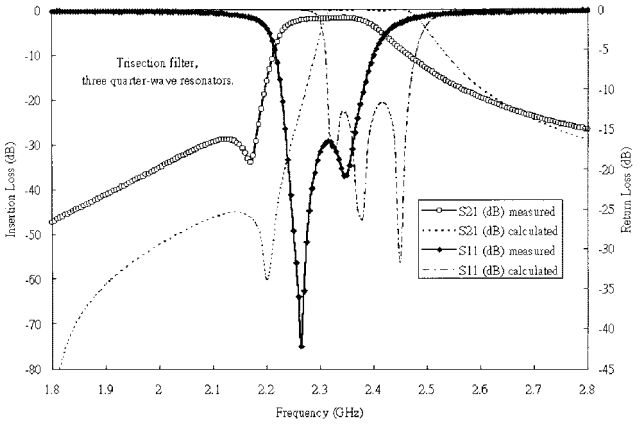

Fig. 12. Calculated and measured results for trisection filter in Table I(h).

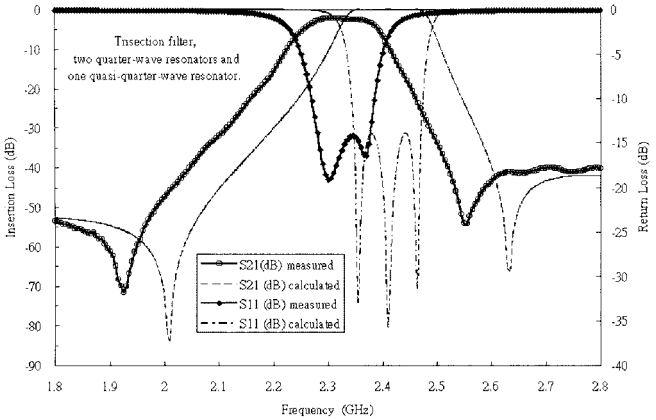

Fig. 13. Calculated and measured results for the trisection filter in Table I(f).

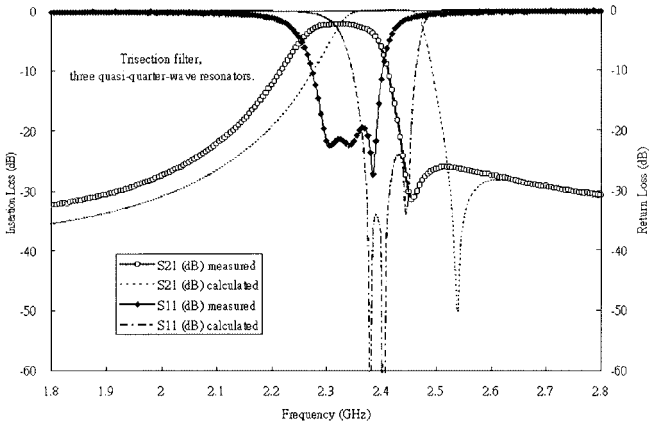

Fig. 14. Calculated and measured results for the trisection filter in Table I(e).

quarter-wave resonator. The finite transmission zero occurs in the lower side of the stopband.

The responses of the four presented trisection filters are all consistent with the prediction (specified OR listed) in Table I.

The measured response of every filter realized in this section is observed to drift toward lower frequencies than the simulated response, possibly because of deviations in dielectric constant and thickness of the substrate. The frequency response drift of the filters realized by quarter-wave resonators is greater than that realized by quasi-quarter-wave resonators. The finding can be explained by the inductance of via-holes. The EM simulation

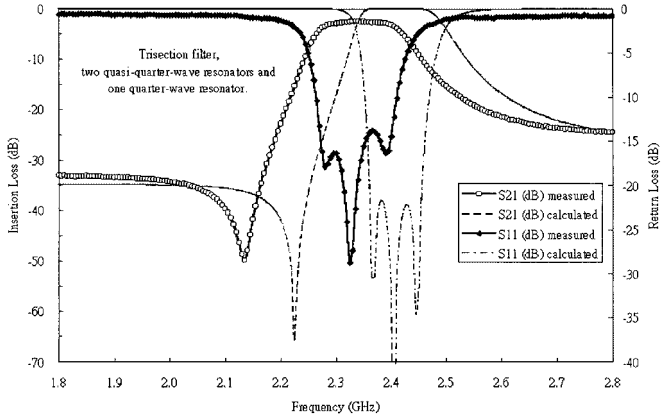

Fig. 15. Calculated and measured results for the trisection filter in Table I(g).

uses a 16 mil $\times$100 mil rectangular via-hole to short the quarter-wavelength resonators, while the short circuit is implemented by two round via-holes with diameters of 16 mil. Two via-holes are in the corners of the strips of the short-circuit end, as shown in Fig. 8(b). Two via-holes contribute greater parasitic inductance than the rectangular via-hole and cause the resonance to drift to lower frequency.

Another practical issue is the sensitivity of the filter response determined by fabrication tolerances. Control of manufacturing variables such as slot width, cross-coupling gap width, and distance between resonators is somewhat limited. Yield analysis has been performed using a circuit simulator such as Microwave Office from Applied Wave Research Inc., Segundo, CA, to evaluate the sensitivity of a filter's response to the deviation of those variables. The simulated results show that the yield rate of a quasi-quarter-wave filter is a little less than that of a quarter-wave filter if the tolerance of the distance between the resonators is constant because the filter that uses quasi-quarter-wave resonators is more compact than that uses quarter-wave resonators. If fabrication tolerances are constant , then the sensitivity of the response of the proposed filters to that previously reported for the cross-coupled filter that uses open-loop or hairpin resonators is around the same level.

V. Conclusion

A new class of miniaturized microstrip cross-coupled filters has been presented to include both the CQ and trisection filters. The use of a quarter-wave resonator and the newly proposed quasi-quarter-wave resonator makes filter configuration very compact. Various responses of CQ and trisection filters are obtained ensuring a proper combination of quarter-wave and newly proposed quasi-quarter-wave resonators.

The filtering characteristics of each filter configuration have been demonstrated as being determined by the phase difference between the main-coupling and cross-coupling paths. The phase relationship of each coupling structure at frequencies below and above the center frequency has been studied using a circuit simulator to determine the total phase shift along the main-coupling and cross-coupling paths.

The quarter-wave resonator and quasi-quarter-wave resonator have a phase difference of 180° when coupled to other resonators. Replacing any resonator with another type causes the phase of the main-coupling path to change by 180° with respect to the cross-coupling path. The same procedure is useful in designing all types of responses of the trisection filter or CQ filter, as presented in this paper.

References

[1] G. L. Matthaei, L. Young, and E. M. T. Jones, *Microwave Filters, Impedance Matching Networks, and Coupling Structures*. Norwood, MA: Artech House, 1980.

[2] S. J. Yao, R. R. Bonetti, and A. E. Williams, "Generalized dual-plane multicoupled line filters," *IEEE Trans. Microwave Theory Tech*, vol. 41, pp. 2182–2189, Dec. 1993.

[3] J. S. Hong and M. J. Lancaster, "Development of new microstrip pseudo-interdigital bandpass filters," *IEEE Microwave Guided Wave Lett.*, vol. 5, Aug. 1995.

[4] G. L. Matthaei, N. O. Fenzi, R. J. Forse, and S. M. Rohlfing, "Hairpin-comb filters for HTS and other narrow-band applications," *IEEE Trans. Microwave Theory Tech*, vol. 45, pp. 1226–1231, Aug. 1997.

[5] P. L. Field, I. C. Hinter, and J. G. Gardiner, "Asymmetric bandpass filter using a novel microstrip structure," *IEEE Microwave Guided Wave Lett.*, vol. 2, pp. 247–249, June 1992.

[6] C. C. Yang and C. Y. Chang, "Microstrip cascade trisection filter," *IEEE Microwave Guided Wave Lett.*, vol. 9, pp. 271–273, July 1999.

[7] J. S. Hong and M. J. Lancaster, "Microstrip cross-coupled trisection bandpass filters with asymmetric frequency characteristics," *Proc. Inst. Elect. Eng.*, pt. H, vol. 146, Feb. 1999.

[8] ——, "Couplings of microstrip square open-loop resonators for cross-coupled planar microwave filters," *IEEE Trans. Microwave Theory Tech*, vol. 44, pp. 2099–2108, Dec. 1996.

[9] ——, "Theory and experiment of novel microstrip slow-wave open-loop resonator filters," *IEEE Trans. Microwave Theory Tech*, vol. 45, pp. 2358–2365, Dec. 1997.

[10] ——, "Cross-coupled microstrip hairpin-resonator filters," *IEEE Trans. Microwave Theory Tech*, vol. 46, pp. 118–122, Jan. 1998.

[11] J. T. Kuo, M. J. Maa, and P. H. Lu, "A microstrip elliptic function filter with compact miniaturized hairpin resonators," *IEEE Microwave Guided Wave Lett.*, vol. 10, pp. 94–95, Mar. 2000.

[12] K. S. K. Yeo, M. J. Lancaster, and J. S. Hong, "The design of microstrip six-pole quasi-elliptic filter with linear phase response using extracted-pole technique," *IEEE Trans. Microwave Theory Tech*, vol. 49, pp. 321–327, Feb. 2001.

[13] S.-Y.Sheng-Yuan Lee and C.-M.Chih-Ming Tsai, "New cross-coupled filter design using improved hairpin resonators," *IEEE Trans. Microwave Theory Tech*, vol. 48, pp. 2099–2108, Dec. 2000.

[14] J. I. Smith, "The even- and odd-mode capacitance parameters for coupled lines in suspended substrate," *IEEE Trans. Microwave Theory Tech*, vol. MTT-19, pp. 424–431, May 1971.

[15] R. Levy, "Filters with single transmission zeros at real or imaginary frequencies," *IEEE Trans. Microwave Theory Tech*, vol. MTT-24, pp. 172–181, Apr. 1976.

[16] ——, "Direct synthesis of cascaded quadruplet (CQ) filters," *IEEE Trans. Microwave Theory Tech*, vol. 43, pp. 2940–2945, Dec. 1995.

[17] R. S. Kwok and J. F. Liang, "Characterization of high-Q resonators for microwave-filter application," *IEEE Trans. Microwave Theory Tech*, vol. 47, pp. 111–114, Jan. 1999.

[18] R. J. Cameron, "Fast generation of Chebyshev filter prototypes with asymmetrically-prescribed transmission zeros," *ESA J.*, vol. 6, no. 1, pp. 83–95, 1982.

[19] ——, "General prototype network-synthesis method for microwave filters," *ESA J.*, vol. 6, no. 2, pp. 193–206, 1982.

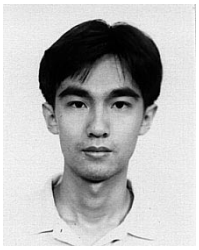

Cheng-Chung Chen was born in Hsinchu, Taiwan, R.O.C., on October 11, 1975. He received the B.S. degree in electrical engineering from the National Sun Yet-Sen University, Kaohsiung, Taiwan, R.O.C., in 1997, the M.S. degree in communication engineering from the National Chiao-Tung University, Hsinchu, Taiwan, R.O.C., in 1999, and is currently working toward the Ph.D. degree in communication engineering at the National Chiao-Tung University.

His research interest is mainly focused on microwave and millimeter-wave circuit design.

Yi-Ru Chen received the B.S. and M.S. degrees in communication engineering from the National Chiao-Tung University, Hsinchu, Taiwan, R.O.C. in 1999 and 2001, respectively.

She is currently a Staff Engineer with Euvis Inc., Westlake Village, CA. Her current research interests include design of high-speed communications integrated circuits (ICs) and printed circuit boards (PCBs).

Chi-Yang Chang (S'88–M'95) was born in Taipei, Taiwan, R.O.C., on December 20, 1954. He received the B.S. degree in physics and M.S. degree in electrical engineering from the National Taiwan University, Taipei, Taiwan, R.O.C., in 1977 and 1982, respectively, and the Ph.D. degree in electrical engineering from the University of Texas at Austin, in 1990.

From 1979 to 1980, he was a Teaching Assistant with the Department of Physics, National Taiwan University. From 1982 to 1988, he was an Assistant Researcher with the Chung-Shan Institute of Science and Technology (CSIST), where he was in charge of the development of microwave integrated circuits (MICs), microwave subsystems, and millimeter-wave waveguide E-plane circuits. From 1990 to 1995, he rejoined CSIST as an Associate Researcher, where he was in charge of development of uniplanar circuits, ultra-broad-band circuits, and millimeter-wave planar circuits. In 1995, he joined the faculty of the Department of Communications, National Chiao-Tung University, Hsinchu, Taiwan, R.O.C., where he is currently a Professor. His research interests include microwave and millimeter-wave passive and active circuit design, planar miniaturized filter design, and monolithic-microwave integrated-circuit (MMIC) design.